ISSN 0020-4412, Instruments and Experimental Techniques, 2013, Vol. 56, No. 3, pp. 256–264. © Pleiades Publishing, Ltd., 2013.
Original Russian Text © M.I. Bryzgunov, A.V. Ivanov, V.M. Panasyuk, V.V. Parkhomchuk, V.B. Reva, 2013, published in Pribory i Tekhnika Eksperimenta, 2013, No. 3, pp. 12–20.

NUCLEAR EXPERIMENTAL TECHNIQUES

A High-Efficiency Collector for a High-Voltage Electron Cooler

M. I. Bryzgunov, A. V. Ivanov, V. M. Panasyuk, V. V. Parkhomchuk, and V. B. Reva

Budker Institute of Nuclear Physics, Siberian Branch,

Russian Academy of Sciences,

pr. Akademika Lavrent'eva 11, Novosibirsk, 630090 Russia

Received April 26, 2012; in final form, July 12, 2012

Abstract—A high-perveance collector with a small secondary emission ratio has been designed for a high-voltage electron cooler. The distinctive feature of this collector is the fact that it consists of the cooled collector itself, which receives the electron flow, and a Wien filter installed ahead of it, which substantially reduces the secondary electron flux emerging from the collector. The main advantage of this design is the combination of the small secondary emission ratio and the high perveance with the small size and ease in manufacturing and adjustment. The results of calculations and experimental investigations of the combined collector are presented, and its different operating modes are investigated. The minimum attained secondary emission ratio is 5×10^{-6}. The methods for further reducing this ratio are proposed.

DOI: 10.1134/S0020441213020048

INTRODUCTION

An electron cooler for an electron energy of 2 MeV is currently developed by the Budker Institute of Nuclear Physics (BINP) for the CO (COoler) SY (SYnchrotron) synchrotron [1, 2]. The COSY synchrotron is intended for experiments with polarized and nonpolarized protons in the energy range of up to 2600 MeV on the internal target or with the beam extraction to the external target. Experiments with the internal target very often require "cooling" of the used beam (i.e., a decrease in the particle momentum spread) in order to suppress the "heating" effects.

Today, two cooling systems have already been used in the COSY synchrotron, which has been reflected in the synchrotron's name. The electron cooling [3] at a low proton energy (50 MeV) provides a means for storing charged particles and increasing its phase density before future experiments. Stochastic cooling [3] impedes degradation in the quality of the beam in its interaction with the target at the energy of an experiment. Unfortunately, stochastic cooling has a natural limitation, which complicates its operation at a high intensity of the cooled beam and a small momentum spread of cooled particles.

Electron cooling at the energy of an experiment will efficiently suppress small-angle scattering and low ionization losses having low probability in interaction of particles with the substance at high energies. Use of it in combination with the stochastic cooling will offer a chance to significantly increase the luminosity of experiments with the internal target.

The schematic diagram of the electron cooler is shown in Fig. 1 on the left, and the layout of the electrostatic accelerator is presented on the right. The stationary electron beam with a current as high as a few amperes is accelerated along electrostatic column *1* and guided over transport system *2* to cooling section *3*, where it moves together with the ion beam (the ion orbit pipe is denoted as *5*). Joint movement results in transfer of the thermal energy from hotter ions to cold electrons.

Having left the cooling section, the electron beam returns back and, over channel *4*, enters the column again, where it loses almost all of the stored energy and is absorbed in the collector. Along its entire path, the beam is kept in the guiding magnetic field. This field sharply increases the efficiency of election–ion interaction in the cooling section, helps to form the required electron beam in the electron gun, and performs transverse beam focusing in the electrostatic column and the transport system.

The main parameters of the electron cooler are as follows:

Energy range, MeV	0.1–2
Energy instability	$<10^{-4}$

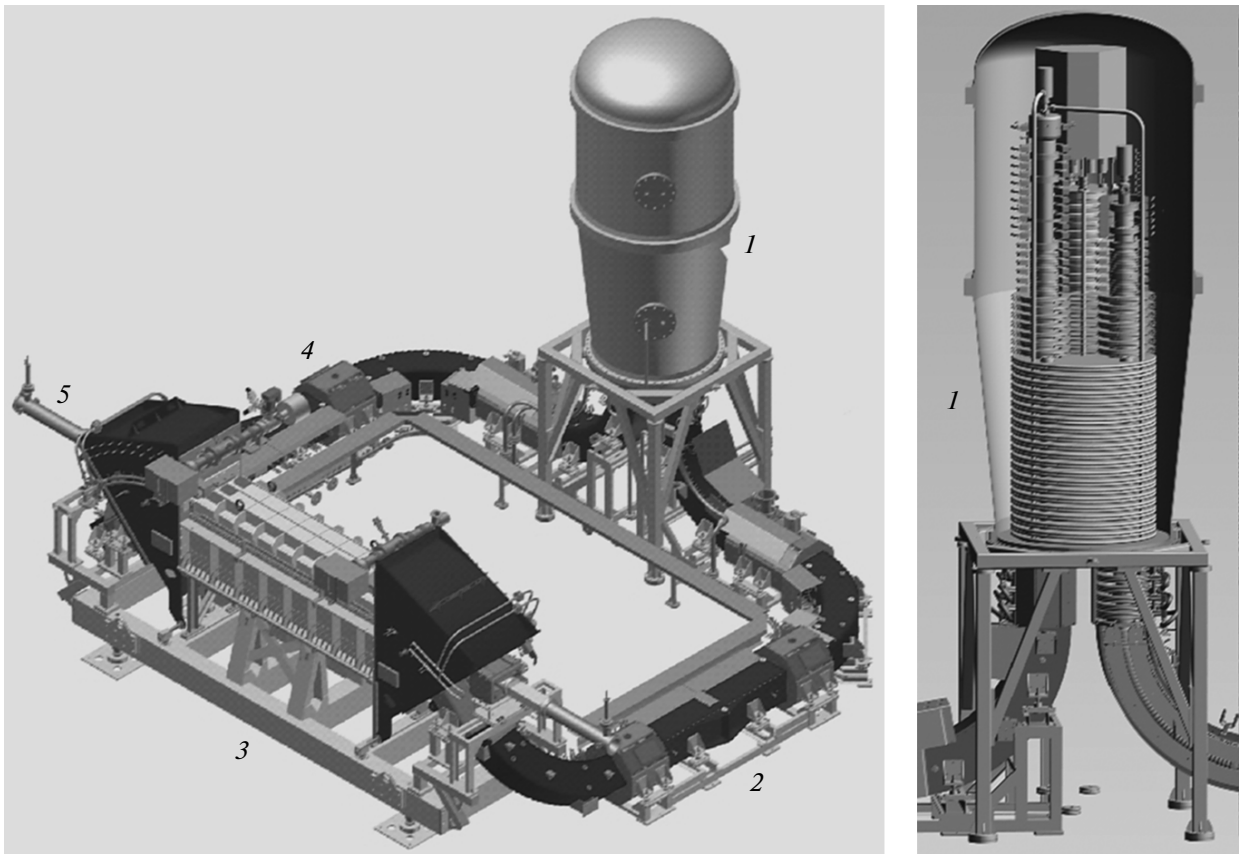

Fig. 1. Schematic diagram of the electron cooler for the COSY synchrotron (left) and external appearance of the electrostatic accelerator (right): (*1*) electrostatic accelerator, (*2*) transport channel to the cooling section, (*3*) ion beam cooling section, (*4*) reverse transport channel, and (*5*) ion channel.

Electron current, A	0.1–3
Electron beam diameter, mm	10–30
Cooling section length, m	2.69
Radius of turns, m	1.00
Magnetic field in the cooling section, kG	0.5–2
Vacuum, mbar	10^{-9}–10^{-10}
Total length along the synchrotron, m	6.39
Maximum height, m	5.7
Height of the proton beam channel, m	1.8

Depending on the initial conditions, the expected cooling rate is $\leq 0.01\ s^{-1}$.

One of the key problems encountered in development of a facility of this type is to maintain the stability of its operation in the deep recuperation mode. For this purpose, it is extremely important that the losses of electrons accelerated to the total energy on the vacuum chamber walls be minimized. In the guiding magnetic field, the primary beam reaches the collector almost without losses. Secondary electrons escaping from the collector are again accelerated along the column and, when the beam is bent in the guiding magnetic field, if no special measures are taken, hit the walls of the chamber (which are at the ground potential) as a result of the centrifugal drift. In this case, they knock out ions, which, in succession, having acquired their total energy, knock electrons out of the walls (which are at the high-voltage potential), thus providing the "current" coupling between the high potential and the ground, which results in a breakdown.

The other breakdown mechanism is associated with charging of the accelerating tube by secondary electrons scattering from inhomogeneities of the optical system. Subsequent equalizing of charges along the accelerating tube, which is followed by a microbreakdown, is capable of initiating a full-voltage breakdown. Experimental data obtained at the Fermilab facility in [4, 5], show that, for the stable operation of the facility to be maintained, the current delivered to the tube must not exceed a few microamperes. Apart from the above problems with the high-voltage stability, losses of accelerated electrons also result in deterioration of the vacuum conditions and an increase in the radiation background around the facility.

In [6], it was shown that, for an axially symmetrical collector, the secondary emission ratio is of the order

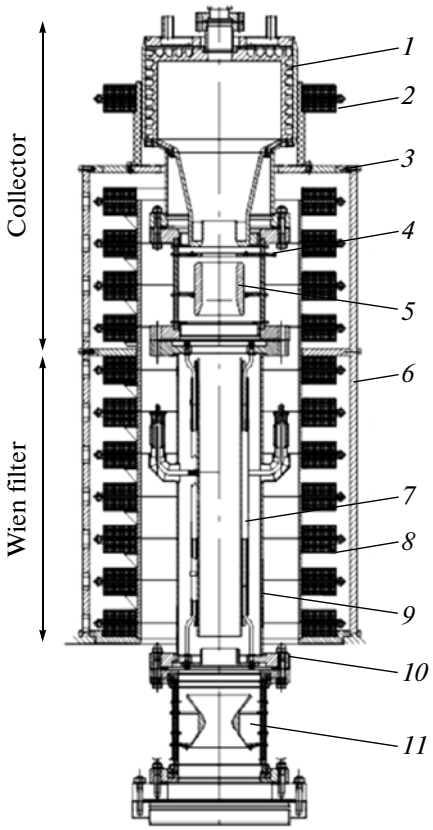

Fig. 2. Schematic diagram of the collector with an analyzing electrode: (*1*) cooled surface, (*2*) collector coil, (*3*) magnetic diaphragm, (*4*) suppressor electrode, (*5*) pre-collector electrode, (*6*) magnetic yoke, (*7*) Wien filter electrostatic plates, (*8*) Wien filter magnetic coils, (*9*) Wien filter vacuum chamber, (*10*) secondary beam diaphragm, and (*11*) analyzing electrode.

of 10^{-4}–10^{-3}. Taking into account the electron beam current, which is a few amperes, it becomes evident that special measures must be taken to substantially reduce the leakage current.

Two methods are used today to reduce the leakage current: implementation of reversible electron motion or the use of a collector with a secondary emission ratio of $\leq 10^{-5}$. The first method implies creation of an electric field at places of beam bending, such that its strength and direction provide full compensation of the centrifugal drift. In this case, the secondary beam travels all its way toward the cathode, is reflected back, again reaches the collector, and is absorbed in it. In this case, the losses are determined by other causes and account for 10^{-5}–10^{-6} of the total beam current. The electrostatic bends were used to good effect in the EC-35, EC-300, and LEIR electron coolers with the maximum electron energy of 35, 300, and 40 keV, respectively [7, 8]. However, as the energy goes up, an increasingly higher electric field is required, which necessitates a significant increase in the voltage applied to the plates of the capacitor producing this field. This fact, together with the considerably increased number of bends, makes the electrostatic drift compensation hard to implement at the facility being designed.

The other approach is to develop a high-efficiency collector with a secondary emission ratio of 10^{-5}, which calls for rejection of the axial symmetry of the magnetic field inside the collector. This may be done using a set of permanent magnets distorting the field lines [9, 10]. In this case, the collector itself is larger-sized and requires careful and laborious adjustment on a special test setup.

COMBINED COLLECTOR

In this paper, we investigate the method for reducing the leakage current from the collector, which was proposed in [11]. It consists in using an axially symmetric collector and a Wien filter placed ahead of it. The Wien filter [12] is a region with crossed transverse electric and magnetic fields selected so that their actions compensate each other for electrons of the primary beam. The secondary electrons moving in opposite direction are strongly deflected from the axis and absorbed by the filter diaphragm that is held at the potential of the vacuum chamber. The diagram of such a combined collector is presented in Fig. 2.

The crossed fields in the Wien filter are formed by electrostatic plates *7* and the transverse magnetic field produced by permanent magnets. The deflected secondary beam deposits on diaphragm *10*. Cooled surface *1* receives the primary electron beam and is expected to scatter a thermal energy of up to 15 kW at a collector current of 3 A (the maximum current mode).

Suppressor electrode *4* is used to produce an electrostatic barrier locking low-energy secondary electrons inside the collector. The suppressor potential is selected to be close to the cathode potential. Though being strongly decelerated near the suppressor, the primary beam passes further; whereas secondary electrons deposit a fraction of their energy in interaction with the collector surface and are reflected back into the collector. Pre-collector electrode *5* also participates in the formation of the electrostatic barrier. At high beam currents (~1 A), its potential is selected to be equal to the collector potential; at lower currents, it is expedient that this potential be decreased. All potentials are produced by sources located in the high-voltage terminal, which are held at the cathode potential.

The final collector coil *2* is connected oppositely to the other coil of the longitudinal magnetic field and, together with magnetic diaphragm *3*, is responsible for a sharp drop of the magnetic field inside the collector. Incidentally, the magnetic barrier is formed; it reflects

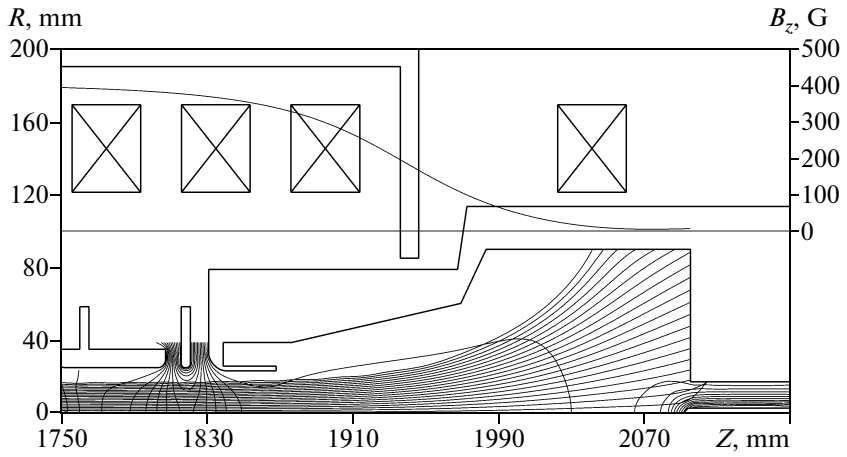

Fig. 3. Inner surface of the collector and the suppressor electrode. The trajectories of primary beam electrons, the equipotential lines with a 100-V step, and the distribution of the magnetic field on the axis are shown.

a portion of secondary electrons with a high transverse energy. Attenuation of the magnetic field also extends the beam, and the current density in it decreases, which prevents local overheating of the collector surface. The coils of the longitudinal magnetic field have the following parameters: inner radius, 12 cm; outer radius, 17 cm; coil thickness, 4 cm; number of turns, 970; maximum current, up to 2.7 A; and coil period in the regular part, 6 cm. The results of the collector calculations performed using the UltraSAM software package [13] are presented in Fig. 3.

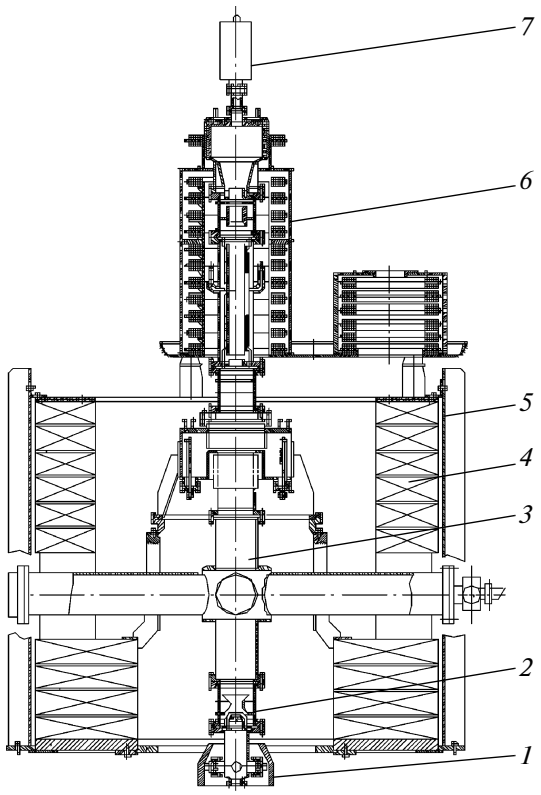

Fig. 4. Schematic diagram of the electron gun–collector test setup: (*1*) magnetic concentrator of the electron gun, (*2*) electron gun, (*3*) drift gap, (*4*) coils of the magnetic system of the gun and drift gap, (*5*) magnetic shield, (*6*) combined collector, and (*7*) vacuum pump.

Note that the secondary electron ratio of the collector required for the correct operation of the Wien filter must be of the order of 10^{-3}, which is readily attainable for an axially symmetric collector. The collector must also satisfy some more requirements. First, the collector perveance must be high enough to intake the maximum current at a minimum collector voltage; otherwise, transmission of a high power to the high-voltage terminal will be required, which is fraught with significant technological difficulties. The calculations have shown that the collector perveance at a completely open suppressor ranges from 13 to 15 $\mu A/V^{3/2}$, depending on the radial distribution of the current density in the electron beam, which is fully adequate for this facility. Second, the collector design must allow removal of a significant fraction of the thermal power. In our facility, the inner surface of the collector is cooled by transformer oil delivered over inner tubes.

A GUN–COLLECTOR TEST SETUP

The combined filter was tested on a special gun–collector setup, the diagram of which is shown in Fig. 4. The beam generated in electron gun *2* passed through drift gap *3* and hit combined collector *6*. Vacuum inside the collector was maintained by ion pump *7*. The magnetic field was ~500 G near the gun and the Wien filter region and ~650 G in the drift gap.

A ceramic insertion with a special analyzing electrode (*11* in Fig. 2) was placed behind the filter. The electrode was installed in place where the magnetic

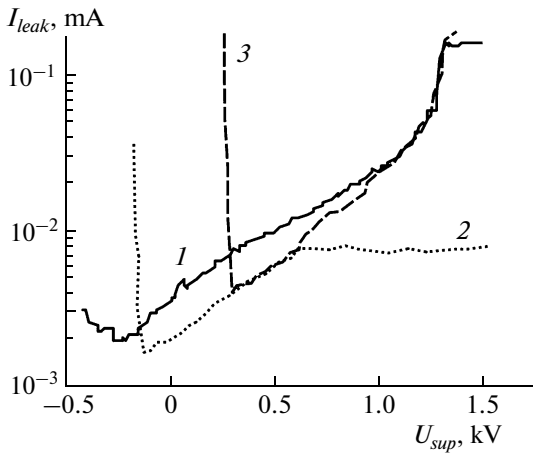

Fig. 5. Dependence of leakage current I_{leak} on suppressor electrode potential U_{sup} for operating modes *1*–*3* with the Wien filter being switched off: (*1*) the pre-collector electrode is connected to the collector; (*2*) the pre-collector electrode has the potential equal to one-half the collector potential; (*3*) the suppressor electrode is connected to the collector, and the cutoff voltage is applied to the pre-collector electrode. The primary beam current is 210 mA, and the collector potential is 1.3 kV.

field had a local minimum, and its diameter was smaller than the diameter of the Wien filter diaphragm. Thus, this electrode was the narrowest section of the entire electron-optical system of the test setup; the secondary electrons that passed through the Wien filter and were deflected in it hit this electrode with a high probability.

COLLECTOR EFFICIENCY IN THE STRAIGHT SYSTEM

Initially, the operating modes of the collector were investigated on the straight system with the Wien filter being switched off. In this case, the test setup is a straight axially symmetric system with a reversible electron dynamics. This mode is equivalent to the mode use for the coolers with the electrostatic drift compensation. An electron reflected from the collector oscillates between the gun and the collector until it is absorbed in the collector or hits the walls of the vacuum chamber. The leakage currents at different operating modes of the collector are shown in Fig. 5. The experimental data are presented for a collector potential of 1.3 kV in order to illustrate the effects associated with the space charge. The working value of the collector potential is in the range of 2.5–5.0 kV.

Analysis of Fig. 5 shows that many secondary electrons gather in the low-energy region (~100 eV), which is responsible for the fast rise in the leakage current in the region $U_{sup} \approx U_{coll}$. The leakage current monotonically decreases as the suppressor potential approaches the cathode potential and the potential barrier for the secondary electrons increases. After reaching a certain minimum value, the leakage current starts sharply growing in value owing to the reflection of the primary electrons from the barrier.

The use of the pre-collector electrode as a suppressor (mode *3*) does not offer significant advantages. It is apparent that, in this case, the leakage current coincides with the current of mode *1* and is substantially lower at the cutoff point. However, the operating region of this mode is rather narrow. Since the pre-collector electrode is much longer than the actual suppressor, the effect of the main beam current cutoff on it is more pronounced.

Mode *2* possesses intermediate properties. At the expense of the additional decrease in the pre-collector electrode potential, the larger portion of the secondary electrons is immediately cut off, and retention of the remaining electrons can be adjusted by varying U_{sup}. In this case, the region of operating parameters for U_{sup} is not as narrow as in mode *3*. The drawback of this mode is the limitation on the maximum current by a value of 1.8 A, which is caused by the inadequate throughput of the pre-collector electrode at a reduced voltage.

COMBINED COLLECTOR EFFICIENCY

After the Wien filter is switched on, the possibility appears of directly measuring the collector efficiency and estimating the Wien filter performance. The leakage current to the vacuum chamber of the Wien filter provides the value of an electron flux reflected from the collector and deflected by the system of the Wien filter fields. Measuring the current arriving at the analyzing electrode allows one to estimate the combined collector efficiency.

The dependence of the leakage current on the value of the electrostatic barrier produced by the suppressor is presented in Fig. 6. It is apparent that introduction of the additional barrier due to the pre-collector electrode positively affects the collector efficiency. The collector efficiency is at a maximum near the threshold of virtual cathode production, when the combined action of the pre-collector electrode and the spatial charge most fully implements electrostatic cutoff of the secondary electrons. Further increase in the cutoff potential results in suppression of recuperation. The minimum values of the secondary emission ratio of the collector range from 5×10^{-4} to 10^{-3} and, for the combined collector, to 5×10^{-6}.

The dependence of the leakage current on the value of the magnetic barrier at the collector input is shown in Fig. 7. The barrier value is regulated by the current in the final coil. It is apparent that there is an optimum at ~2.5 A. The optimum value depends on the collector voltage only slightly. At high current values, stepwise deterioration of the collector performance is observed: an increase in the coil current by 50–100 mA relative to

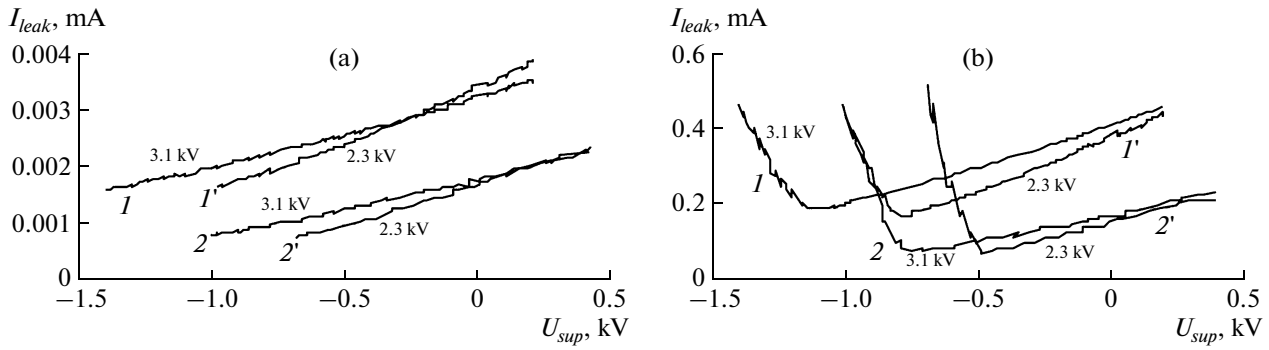

Fig. 6. Dependence of leakage current I_{leak} on suppressor electrode potential U_{sup} at different collector voltages (designated by numbers) for (a) combined collector and (b) collector with the pre-collector electrode held (*1*, *1*') at the collector potential and (*2*, *2*') at one-half the collector potential. The primary beam current is 220 mA.

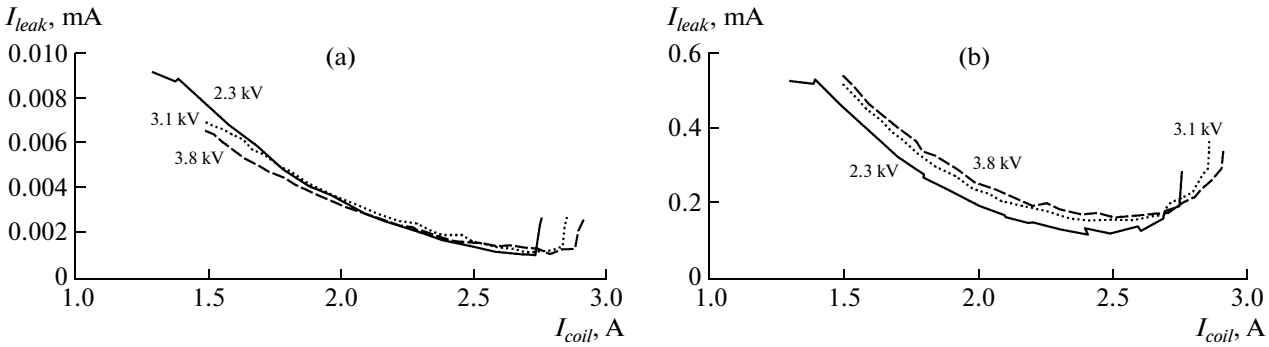

Fig. 7. Dependence of leakage current I_{leak} on collector coil current I_{coll} at different collector voltages (designated by numbers) for (a) the combined collector and (b) collector. The primary beam current is 220 mA.

the maximum values in Fig. 7 results in suppression of recuperation. In this case, electrons of the primary beam start being reflected from the region of a high inverse field without reaching the collector surface (see Fig. 8). As the collector voltage goes down, the limiting coil current weakly decreases. For example, in

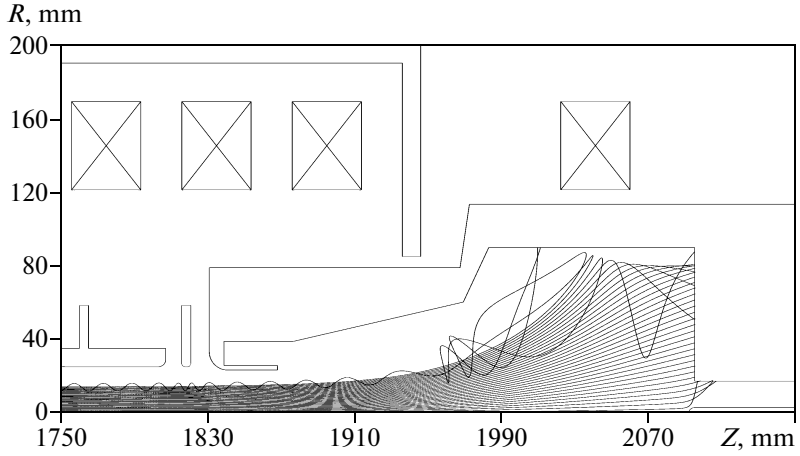

Fig. 8. Reflection of the primary beam electrons at a high current in the collector coil.

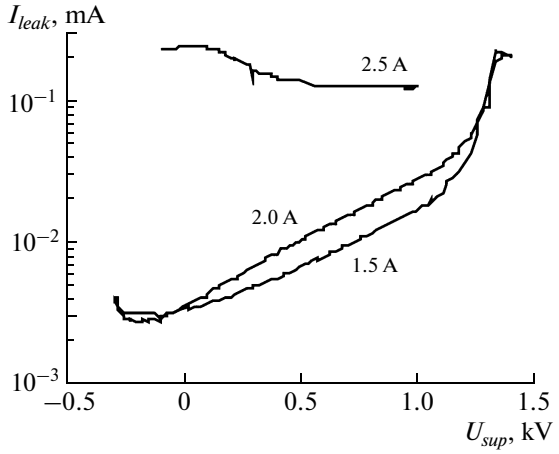

Fig. 9. Dependence of the leakage current on the suppressor electrode potential for different collector coil currents (designated by numbers). $U_{coll} = 1.3$ kV.

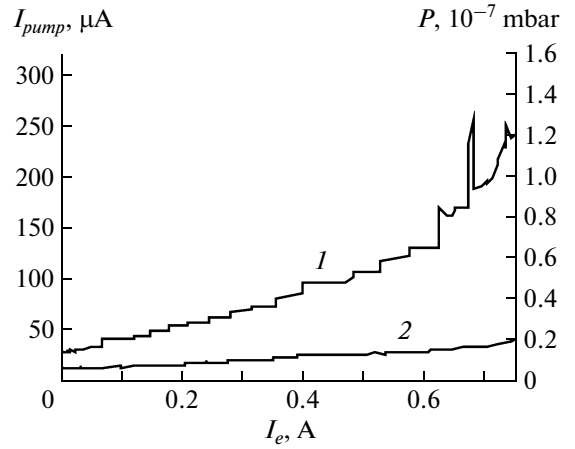

Fig. 11. Vacuum estimated by the change in ion pump current I_{pump} for the modes (*1*) of degradation of the titanium film in the vacuum pump and (*2*) sputtering deposition of a new film. The primary data are the currents from the ion pumps. The pressure was converted by the formula 1/2000 mbar.

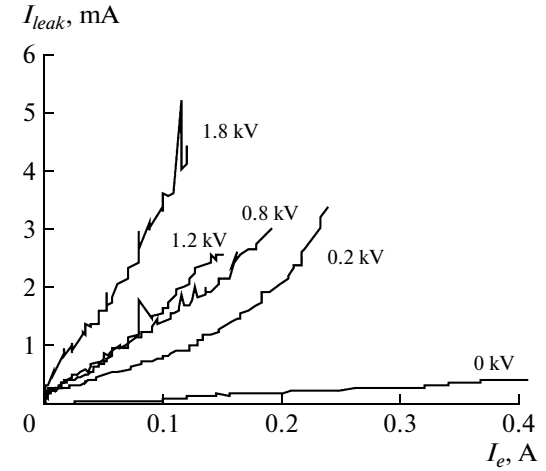

Fig. 10. Leakage currents in the system when the collector is connected to the Wien filter at different potentials ΔU between the vacuum chamber and the capacitor midpoint (designated by numbers).

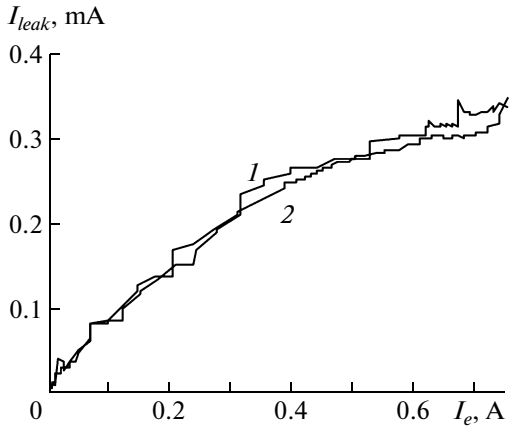

Fig. 12. Leakage current vs. electron beam current I_e for the modes (*1*) of degradation of the titanium film in the vacuum pump and (*2*) sputtering deposition of a new film.

the mode with $U_{coll} = 1.3$ kV, reflection of primary electrons proceeds as early as at a current of 2.5 A (see the respective curve in Fig. 9).

OPERATION OF THE WIEN FILTER AT DIFFERENT VACUUM CHAMBER POTENTIALS

The vacuum chamber of the Wien filter and the diaphragm in it (electrodes *9* and *10* in Fig. 2) are connected together and have an isolated power supply, since they must receive the current of secondary electrons from the collector. In the course of the experiments, we investigated the mode when the potential of these electrodes was equal to the collector potential. The main principle of this mode is the absence of a limit on the leakage current from the collector, since the power supply of the collector in any case receives the total current, the permissible flux of secondary electrons toward these electrodes may take on any value. From the standpoint of electron motion inside the filter, it is assumed that no problem will be encountered. The capacitor midpoint may be held at any potential W and additionally accelerates the beam to the preset energy. In reality, all attempts to implement this mode lead to a significant deterioration in the efficiency of the "collector + Wien filter" system.

Figure 10 presents the leakage currents in the collector + Wien filter system at different potentials ΔU between the vacuum chamber and the capacitor midpoint. The mode $\Delta U = 0$ corresponds to the standard connection. In the variant with $\Delta U = 1.8$ kV, the vac-

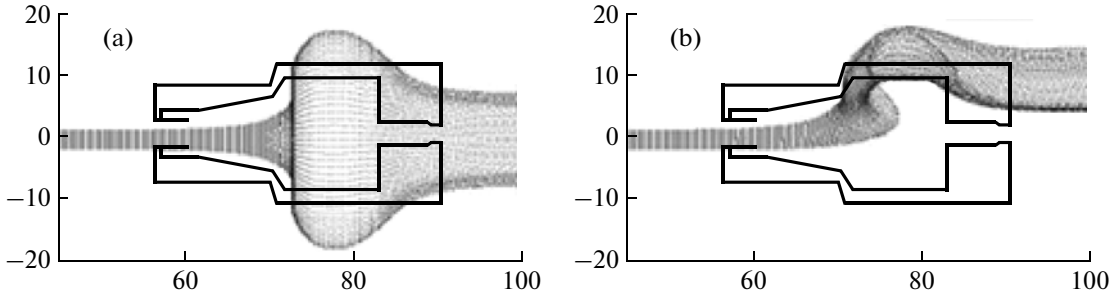

Fig. 13. Distribution of the magnetic field lines (a) in the axially symmetric and (b) asymmetric cases.

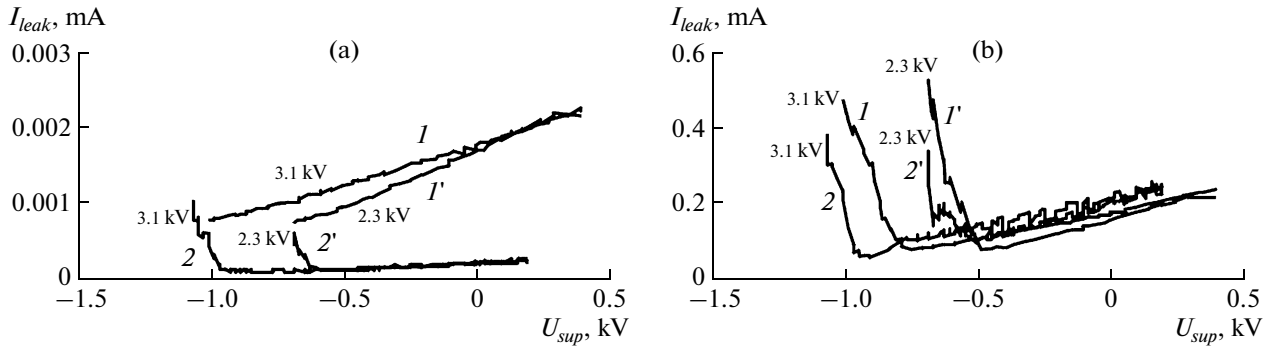

Fig. 14. Leakage current vs. the suppressor electrode potential in the cases (*1*, *1'*) of the axially symmetric and (*2*, *2'*) asymmetric magnetic fields at different collector voltages (designated by numbers) for (a) the combined collector and (b) the collector. The primary beam current is 220 mA.

uum chamber was connected to the collector. In this case, the losses increase considerably, and a high beam current cannot be obtained in the recuperation mode. Therefore, normal operation of the Wien filter requires that the vacuum chamber potential be as close as possible to the midpoint potential of the electrostatic plates. This may be explained by a distortion of the trajectory of the primary beam in its motion at the entrance in the system of electrostatic plates and the exit from it.

COLLECTOR EFFICIENCY AS A FUNCTION OF VACUUM

The vacuum conditions were thought to be among the effects responsible for the leakage current from the collector in [14]. To verify this statement, we performed two sets of measurements of the leakage current and the quality of vacuum as functions of the electron beam current. One set of measurements was taken after a long pause in operation, when the titanium film in the vacuum pump had already been degraded, and the other measurements were performed immediately after the sputtering deposition of the titanium film. Vacuum was estimated by the current in the getter-ion pump, and its dependence on the beam current is presented in Fig. 11. After the film degradation, the appearance of the electron current resulted in vacuum deterioration by factors of 5–6 (curve *1*). If the titanium film was fresh, vacuum degraded considerably weaker (curve *2*). The leakage current is presented in Fig. 12. It is apparent that the vacuum conditions almost do not affect the leakage currents, though the vacuum conditions differ severalfold.

COMBINED COLLECTOR: AN AXIALLY ASYMMETRIC CASE

As mentioned above, the electron flux from the combined collector can be reduced by using a transverse magnetic field in the region near the collector. Electrons reflected from the collector surface cannot return over the same path and behave as though they get entangled in the magnetic field lines, remaining inside the collector. The design of the described collector allows implementation of this mode by removing one half of the magnetic diaphragm. In this case, the axial symmetry of the magnetic field lines is distorted, and the magnetic field lines are displaced toward one side (Fig. 13).

The dependences of the leakage currents for two operating modes of the collector are compared in Fig. 14. Analysis of these curves shows that the magnetic bending has almost no effect on the collector efficiency, but the efficiency of operation of the combined collector increases sharply.

This result can be explained by the fact that the collector used in this study has not been designed for operation with a bend inside it. For a collector with a bend, the important condition for efficient suppression of the secondary electron flux is its shift by the value that is approximately equal to the sum of the beam radius and the radius of the collector inlet [10]. The shift of both the primary and secondary beams proceeds by centrifugal drift in their passing through the bending field of the collector.

For the asymmetric operating mode of the collector, the beam shift (which is equal to the shift of the primary beam plus the shift of the secondary one) is ~1.5 cm. At a 2.5-cm radius of collector inlet, this means that the collector efficiency improves only slightly. However, since the beam is nevertheless shifted, if the directions of shift inside the collector and the Wien filter coincide, the beam is more strongly deflected toward the secondary collector, thus improving the efficiency of the combined collector.

CONCLUSIONS

A combined collector of the stationary electron beam consisting of the Wien filter and the axially symmetric collector itself for the high-voltage electron cooler have been designed and tested. In the course of the experiments, different operating modes of the combined collector have been investigated, and a very small (5×10^{-6}) secondary emission ratio of the collector has been obtained. This small ratio, together with the high perveance, a small size, and ease in manufacturing and adjustment suggest that this collector is optimum for use in the high-voltage electron cooler.

ACKNOWLEDGMENTS

This work was supported by the Ministry of Education and Science of the Russian Federation and the Federal Target Program "Human Capital for Science and Education in Innovative Russia" for 2009–2013 (state contract nos. P1198 and 02.740.11.0513).

REFERENCES

1. Dietrich, J., Kamerdzhiev, V., Bryzgunov, M.I., et al., *Proc. COOL'-09*, Lanzhou, China, 2009, p. 178.
2. Alinovsky, N., Batrakov, A.M., Bedareva, T.V., et al., *Proc. COOL'-11*, Alushta, Ukraine, 2011, p. 37.
3. Skrinskii, A.N. and Parkhomchuk, V.V., *Fiz. Elem. Chast. At. Yadra*, 1981, vol. 12, no. 3, p. 557.
4. *HESR Electron Cooler. Design Study*, Uppsala: The Svedberg Laboratory Uppsala University, 2009.
5. Prost, L.R. and Shemyakin, A., *Proc. AIP Conf. COOL'-05*, Galena, USA, 2005, vol. 821, p. 391.
6. Sharapa, A.N. and Shemyakin, A.V., *Nucl. Instrum. Methods Phys. Res., A*, 1994, vol. 351, p. 295.
7. Bocharov, V., Bubley, A., Boimelstein, Yu., et al., *Nucl. Instrum. Methods Phys. Res., A*, 2004, vol. 532, p. 144.
8. Bubley, A., Parkhomchuk, V., Reva, V., et al., *Proc. RuPAC-06*, Novosibirsk, 2006, p. 25.
9. Sharapa, A., Shemyakin, A., and Nagaitsev, S., *Nucl. Instrum. Methods Phys. Res., A*, 1998, vol. 417, p. 177.
10. Prost, L.R. and Shemyakin, A., *Proc. PAC-05*, Knoxville, USA, 2005, p. 2387.
11. Meshkov, I.N., Salimov, R.A., and Fainshtein, V.G., *Zh. Tekh. Fiz.*, 1973, vol. 43, no. 8, p. 1782.
12. Ivanov, A.V., Bryzgunov, M.I., Bubley, A.V., et al., *Proc. RuPAC-10*, Protvino, Russia, 2010, p. 233.
13. Ivanov, A.V. and Tiunov, M.A., *Vestnik Novgorod. Gos. Univ. Ser.: Fizika*, 2008, vol. 3, no. 1, p. 56.
14. Bosser, Zh., Bykovskii, V.F., Lei, R., et al., *Preprint of Inst. Nucl. Phys. Sibir. Branch Russ. Acad. Sci.*, Novosibirsk, 1991, no. 25.

Translated by N. Goryacheva